A Prototype Personal Navigation System

Wayne Soehren and Wes Hawkinson
Honeywell Advanced Technology
3660 Technology Drive
Minneapolis, MN 55418
USA

wayne.soehren@honeywell.com
wes.hawkinson@honeywell.com

ABSTRACT

Honeywell Laboratories recently funded the development of a prototype personal navigation system based on MEMS technologies. The system components include an MEMS inertial measurement unit, a three-axis magnetometer, a barometric pressure sensor, and a SAASM GPS receiver. The system also uses Honeywell's human motion-based pedometry algorithm. The navigation process is based on a strap-down inertial navigator aided by feedback from a Kalman filter using typical measurements from the GPS, magnetometer and barometer when available. A key innovation is the addition of an independent measurement of distance traveled based on use of a human motion algorithm. The navigation system combines the best features of dead reckoning and inertial navigation, resulting in positioning performance exceeding that achieved with either method alone.

Subsequent to the Honeywell effort, DARPA funded an individual Personal Inertial Navigation System (iPINS) seedling program. Honeywell worked to improve the baseline personal navigation system with the objective of demonstrating the feasibility of reliably achieving navigation accuracy < 1% of distance traveled in GPS-denied scenarios. In addition, an analysis was conducted to determine the benefit of incorporating terrain correlation into the personal navigation system. The results of this analysis indicate that overall navigation accuracy can be significantly improved through the application of terrain correlation.

This paper presents an overview of Honeywell Laboratories' prototype Personal Navigation system, the software architecture, and the personal navigation algorithms. Demonstration results from the DARPA iPINS seedling program are presented. In addition, the paper includes the conclusions from the terrain correlation analysis conducted under the iPINS seedling program

1.0 INTRODUCTION

One of the most challenging and as yet unsolved problems for dismounted soldiers is accurate geolocation, necessary to maintain situational awareness and to supply accurate targeting information for smart weapons. Although soldiers carry GPS equipment for navigation, GPS performance significantly degrades in urban canyons, indoor/underground facilities and thickly foliated areas. Low-cost inertial/GPS-based navigation systems provide short-term performance improvement, but long-term performance in GPS-denied areas does not meet current or future mission requirements. There is a clear need for a lightweight, low-power personal navigation system that provides accurate geolocation that has low dependence on external reference sources, such as GPS.

2.0 PERSONAL NAVIGATION SYSTEM OVERVIEW

The prototype system shown in Figure 1 was developed under Honeywell IR&D and consists of a Honeywell BG1930 MEMS Inertial Measurement Unit (IMU), a Rockwell Collins NavStorm GPS receiver, a Honeywell designed processor, a Honeywell HMR3300 magnetometer, and a Honeywell Precision Altimeter (HPA). The processor was originally designed for the BG1920 Flight Management Unit (FMU), a prototype MEMS GPS/INS demonstrated on a number of projectile and UAV applications. The NavStorm GPS receiver and processor are packaged together, as shown in Figure 1

A system interface assembly (labeled the Mini PING) was developed to provide power management, interface signal translation (i.e. RS-232 to RS-422), and a break out capability to allow various signals to be monitored. In addition, a handheld remote unit was built to allow the system to be easily powered on and off, and to provide some limited discrete I/O capability to the user. The discretes were used to allow the user to place the system in calibration mode, enable/disable use of GPS aiding, and to "mark" an event. LEDs on the Remote Unit were used to reflect system status (i.e. GPS in use, mark input received, and barometer/magnetometer operational).

3.0 SOFTWARE ARCHITECTURE & ALGORITHMS

Software for the iPINS system was developed using Honeywell Labs' ECTOS™ IIc software package. Honeywell has expanded on Honeywell's Ada ECTOS™ II software package, creating the ECTOS™ IIc software package based on the C++ programming language. ECTOS™ IIc was designed to enable rapid development of new applications for Honeywell's BG19XX FMU. To achieve this goal, a hierarchical software structure was chosen for ECTOS™ IIc, shown in Figure 2.
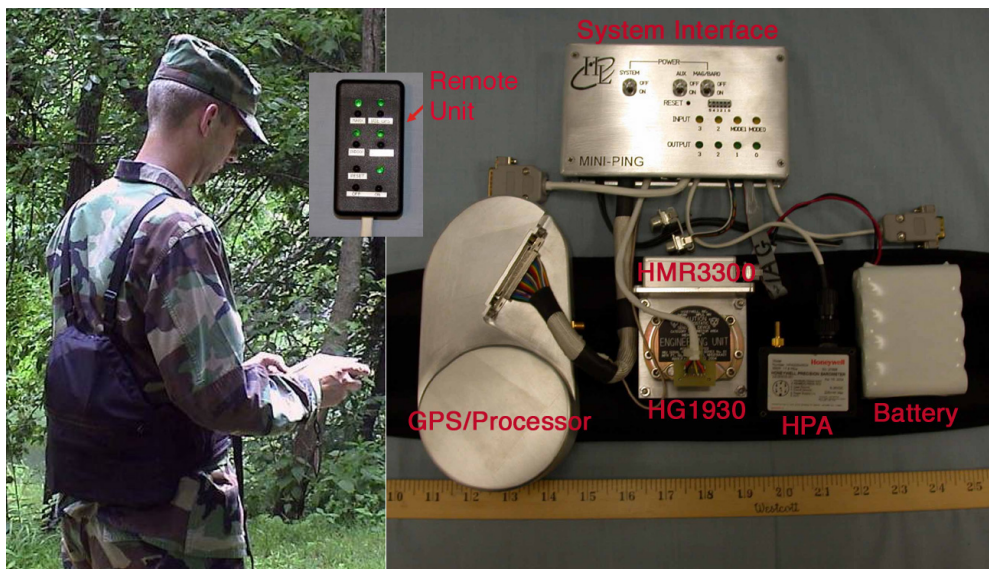

Figure 1. Prototype individual Personal Inertial Navigation System (iPINS)

A functional block diagram of the demonstration system is shown in Figure 3. Honeywell's human motion algorithm models four motion types or classes: 1) walking forward, 2) walking backward, 3) running, and 4) stopped. The motion classification algorithm is essentially a two-step process: first, identify the motion class, and then, estimate the distance travelled based on the identified motion class. When coupled with heading, the estimate of position displacement formed is usable as a measurement to the Kalman filter.

The walking forward model, shown in Equation 1, was developed previously at Honeywell. This model uses the step period (i.e. time between footfalls, detected in the vertical acceleration) to estimate the step length. This model is easily calibrated by the Kalman filter when external aids, such as GPS, are available.

$$dl = \frac{l_0 dt_s}{dt_s - S}$$

Where

$dl =$ step length

$dt_s =$ time period of step

l_0 and S are step model parameters, unique for each individual and also vary with motion type (walk vs. run)

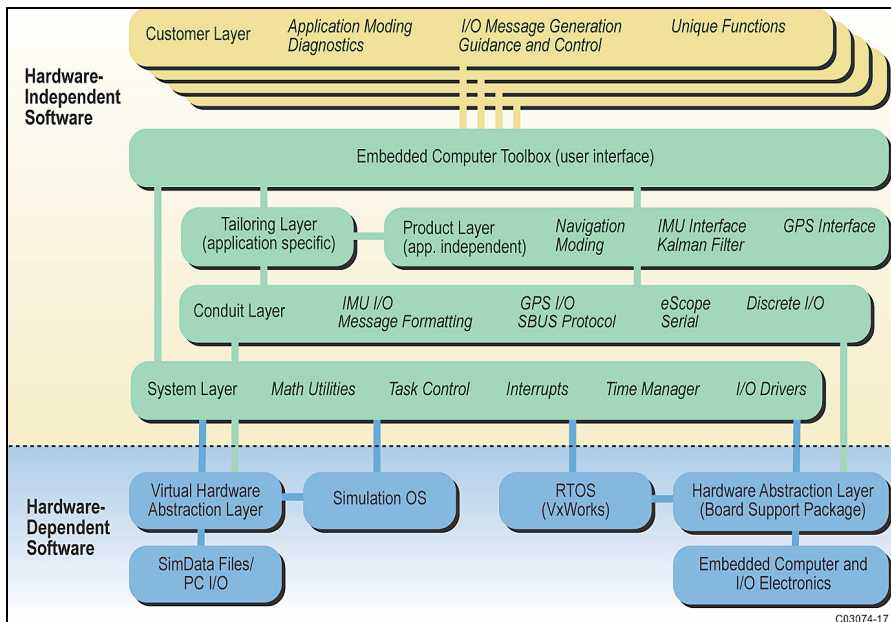**Equation 1. Walking Model Distance Traveled Estimate**

Figure 2. Embedded Computer Toolbox and Operating System (ECTOS™ IIc) Hierarchical Structure
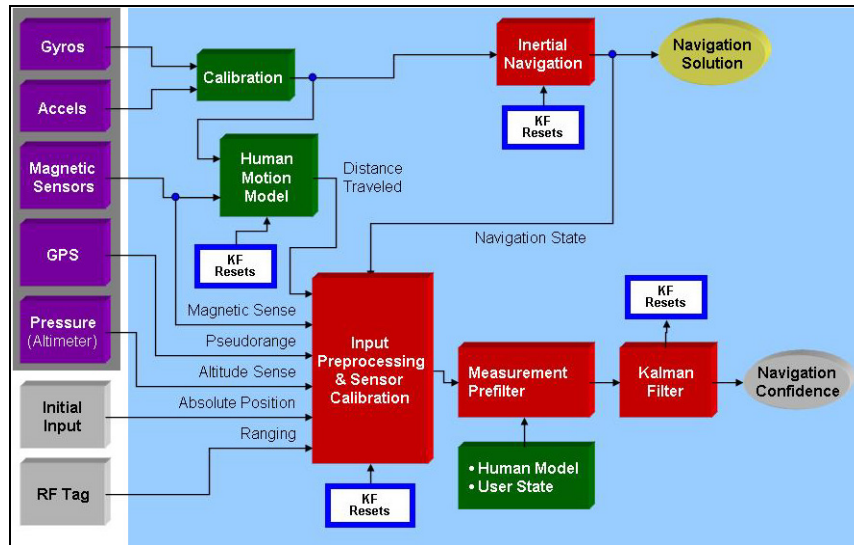
Figure 3. Functional block diagram of iPINS demonstration system

The walking backward model uses the same model as forward walking, but scaled by a factor in the range of 0.75-0.85, that also varies with individual users. Since walking backward is not typically engaged in for an extended period of time, this scale factor was not estimated by the Kalman filter, but was set to a constant value. This state could be added to the Kalman filter in the future to improve performance for backward motion.

The running model was developed based on a literature search and data collected on a treadmill and outdoors. The data suggested that running could be modeled similarly to walking, but with different model parameters. Also, while the model was relatively linear over a range of running speeds (on the order of 3-10 mph), the model is not accurate for sprinting.

Figure 5 shows an example of the treadmill data. The data was collected for a subject that started out walking, ramping up the speed periodically, to the point where the subject was forced to run to remain on the treadmill. The speed was continually ramped up until the subject could no longer safely increase the speed, at which time the speed was ramped down. For this data set, the subject's maximum speed was 9.5 mph, as indicated by the treadmill display. The starting speed was 2.5 mph, and the subject ended with a cool down speed of 2.0 mph. The treadmill speed was changed in 0.5 mph increments.

To test the importance of discriminating between running and walking, model parameters for both the running and walking model were derived from the treadmill data. The step time data was applied to the models; the predicted speeds are shown in Figure 6.

The results show that the walking and running models predict significantly different speeds. During this test, the subject switched from walking to running when the treadmill speed was changed from 4.5 to 5.0 mph, and there is a very noticeable jump at that point. Likewise, on the ramp down from running to walking, which occurred between 4.5 and 4.0 mph, there is a step change in both models. It is clear that motion class should be carefully determined so the correct model can be applied.

This "jump" is also very noticeable in Figure 5b, which depicts the step period measured during the treadmill data collection. This is intuitively obvious; when attempting to walk faster, the stride lengthens and the step frequency increases. When this stride length becomes uncomfortable to maintain, the individual begins running, decreasing the step length and further increasing the step frequency. For the subjects tested, the transition from walking to running was in the range of 4 to 5.0 mph. For the majority of the subjects, this transition corresponded to a step time of 0.4 sec (i.e. step times <0.4 sec were running, >0.4 sec were walking), however this was not a hard threshold.

Honeywell's motion class detector is based on the relatively sharp change in the step time characteristic. Equation 2 describes the method used to determine the threshold step time used to discriminate between running and walking.

$$dt_{threshold} = \frac{\left(\dfrac{l_{0walk}}{2.12344 \text{ m/s}} + S_{walk}\right) + \left(\dfrac{l_{0run}}{2.12344 \text{ m/s}} + S_{run}\right)_s}{2}$$

Where

$dt_{threshold}$ is the step time threshold between walking and running

$l_{0\ run}$ and S_{run} are the running model parameters

$l_{0\ walk}$ and S_{walk} are the walking model parameters

The threshold speed used was 2.12344 m/s, or 4.75 mph

Equation 2.   Walking vs. Running Class Discriminator

Another key element of the motion classification algorithm is the detection of the direction of travel (i.e. forward, backward, or stopped). In the prototype personal navigation system, this was done by differencing the heading, as computed by the strapdown navigation processing, to the direction of position change. Position change direction is computed by differencing the navigation position at the start and end of a step. The direction of motion is determined from the quadrant in which this difference angle lies, as shown in Figure 4.
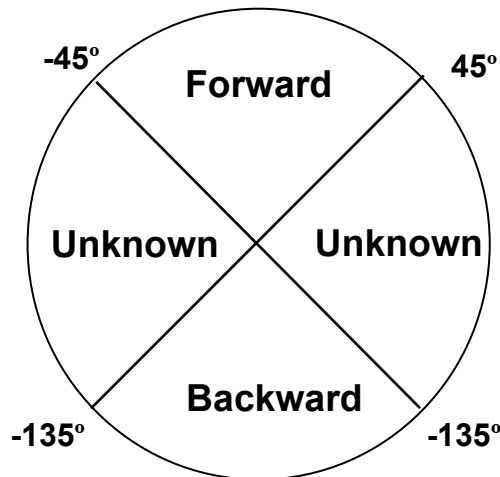

Figure 4. Direction of Motion Determination

When the direction of motion is in the "Unknown" quadrants, motion classification measurements are not processed by the system, and the navigation is operated in the "free inertial" mode. In the future, Honeywell expects to develop a side stepping model to allow more robust motion classification aiding.

4.0   IPINS DEMONSTRATION RESULTS

The iPINS System Demonstration was held at Wright-Patterson Air Force Base. The demonstration was conducted on three scenarios: 1) urban canyon, 2) forested area, and 3) indoors. Wright-Patterson personnel chose the paths and surveyed reference points for each scenario in advance.

4.1 Urban Canyon Scenario

Figure 7 shows the area of Wright-Patterson AFB used for the urban canyon scenario, along with the surveyed reference points. Four individuals walked the course, two at a time. For three of the four trials, GPS was disabled, using the handheld controller "Disable GPS" pushbutton, at the first reference point. On one of the three tests without GPS, the battery failed approximately halfway through the walk.

Figure 8 is a plot of the results for the runs that were completed. The error at each reference point was computed between the navigation systems reported position and surveyed position, provided by the Wright-Patterson personnel. Of interest is the plot for Randy, in yellow. Randy was the user that had GPS enabled throughout the course. Note the large errors between reference marks 30 and 40. This is most likely caused by the effect of multipath on the GPS. The results for the users that did not have GPS enabled are shown in Table 1.

4.2 Forest Scenario

Figure 9 shows the area of Wright-Patterson AFB, including the surveyed reference points used for the forest scenario. Three individuals walked the course with GPS disabled (using the handheld controller "Disable GPS" pushbutton) at the first reference point. The users walked in a normal manner. For this scenario, the distance that GPS was unavailable was approximately 1100 meters. The results are plotted in Figure 10. Table 2 shows the percent of distance traveled error, based on the error at the surveyed points.
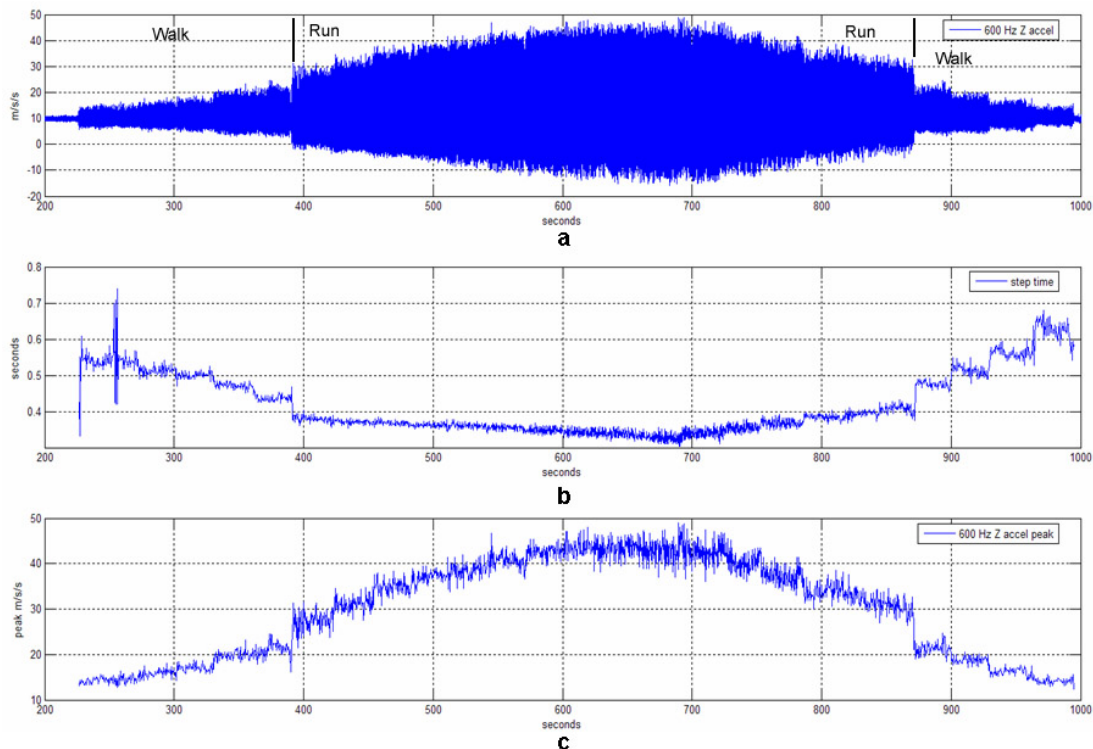

Figure 5. Treadmill Data: a) Raw vertical acceleration, b) Step period, c) Vertical acceleration positive envelope
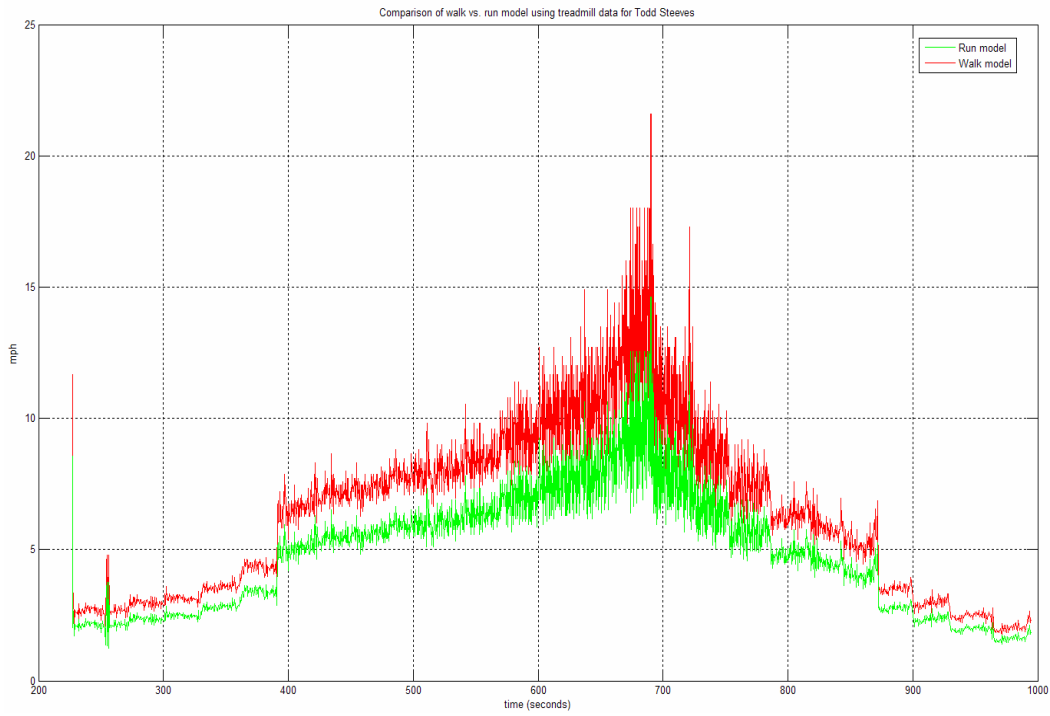
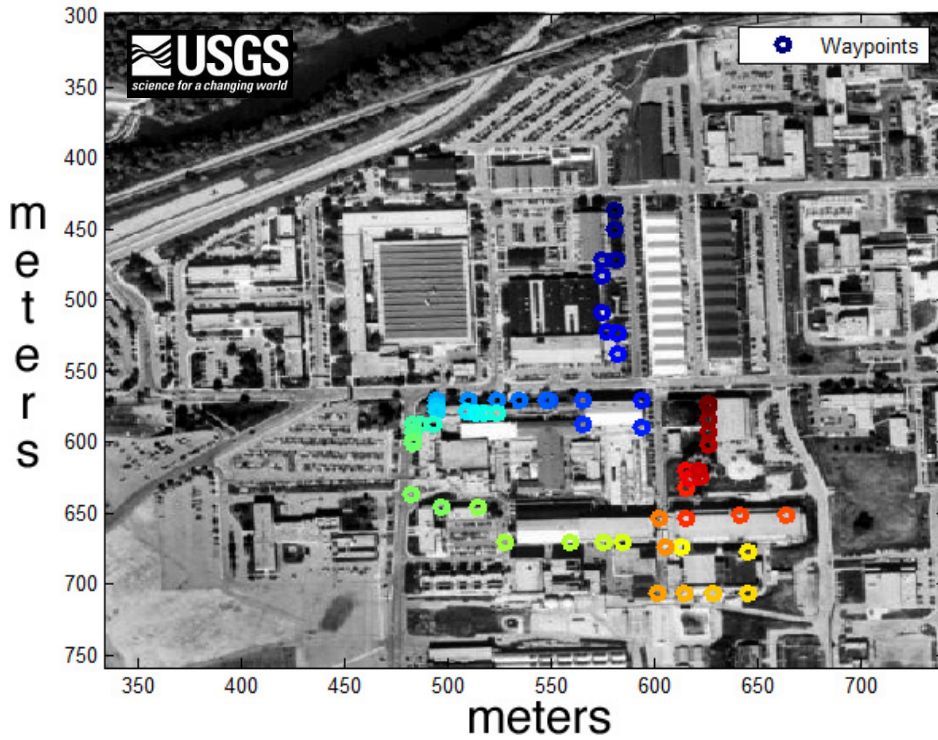Figure 6. Application of walking (red) and running model (green) to treadmill data

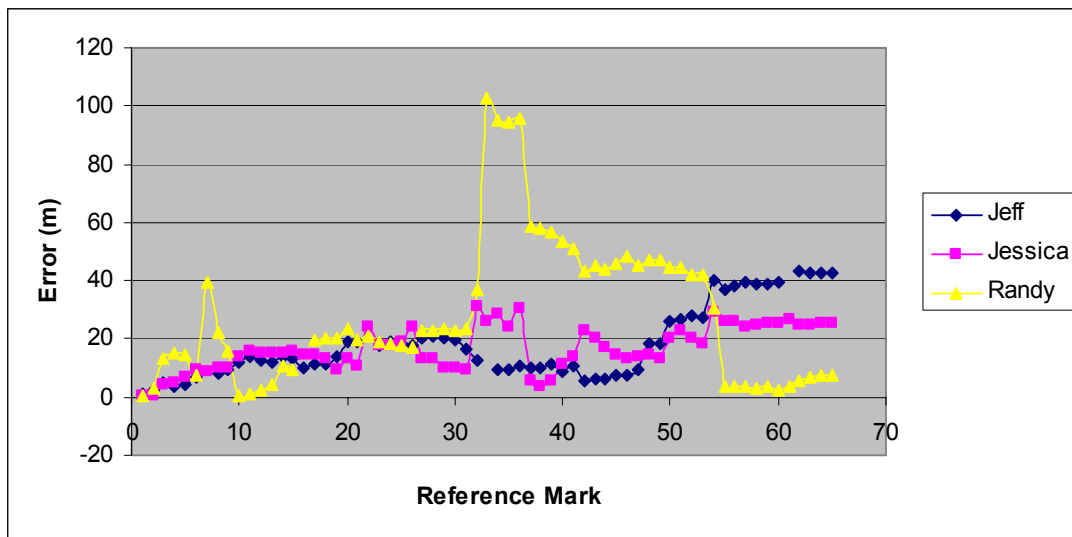Figure 7. Surveyed reference points for urban canyon scenario

Figure 8. Summary of urban canyon results. Yellow plot is for user with GPS enabled throughout the walk.

Table 1. Urban Canyon Final Error

Test Subject	Final error	% Distance traveled (2400 meter)
Jeff	42.72 m	1.78 %
Jessica	25.15 m	1.05 %

4.3   In-building Scenario

Figure 11 shows the area of Wright-Patterson AFB, including the surveyed reference points, used for the in-building scenario. Five individuals walked the course, with two people walking the course twice. The users started outside with GPS enabled, and walked a short distance for initial calibration before entering the building. In general, GPS was not intentionally disabled when the building was entered, since GPS was expected to be blocked when in the building.

The path in the building was routed over three floors of the building, going both up and down stairs. The total length of the path was approximately 700 meters, and time in the building was in the range of 500-600 seconds.

Note that the software used for the demonstration did not have a specific algorithm to identify and model going up or down stairs.

The results of the runs relative to the surveyed in-building path are shown in Figure 12. Table 3 shows the percent of distance traveled error, based on the error at the surveyed points. The results indicate position error growth that is consistent with prior data, but with a higher variation.

Demonstration Conclusions

Overall, the results of the demonstration are encouraging. The primary objective of the seedling (demonstrate the feasibility of achieving 1% distance travelled) was successfully accomplished. Performance in this range, or better, was demonstrated in each of the scenarios, including the indoor scenario for which the system has not been optimized.

5.0 TERRAIN CORRELATION FEASIBILITY STUDY

The feasibility of using terrain correlation as a navigational aid was studied in Phase I of the iPINS program. Terrain correlation navigation primarily depends on the following factors: 1) map accuracy and resolution, 2) terrain suitability, 3) altitude sensor error characteristics and 4) navigation drift between terrain correlation updates. The feasibility study attempted to characterize accuracy of the terrain navigation position updates as a function of terrain characteristics, altitude sensor noise and distance traveled.

5.1 Methodology

The existing iPINS simulation was used as a baseline for the study. Additional components were added as follows:

1) Simulated walking trajectory: A trajectory was generated to represent a walking pace. Since terrain correlation in not dependent on the trajectory dynamics, the trajectory was kept as simple as possible. The resulting trajectory was a straight path due north, with a velocity of 1.25 m/sec.

2) iPINS navigation error model: The iPINS navigation employs a step model to bound free inertial navigation errors to approximately 1% of distance traveled. A distance dependent error model was added to the iPINS simulation to create this effect.

3) Terrain correlation algorithms: Based on the Honeywell-developed PTAN terrain aided navigation system, terrain correlation algorithms were added to the iPINS simulation. The algorithm is based on a Minimum Absolute Difference (MAD) correlator.
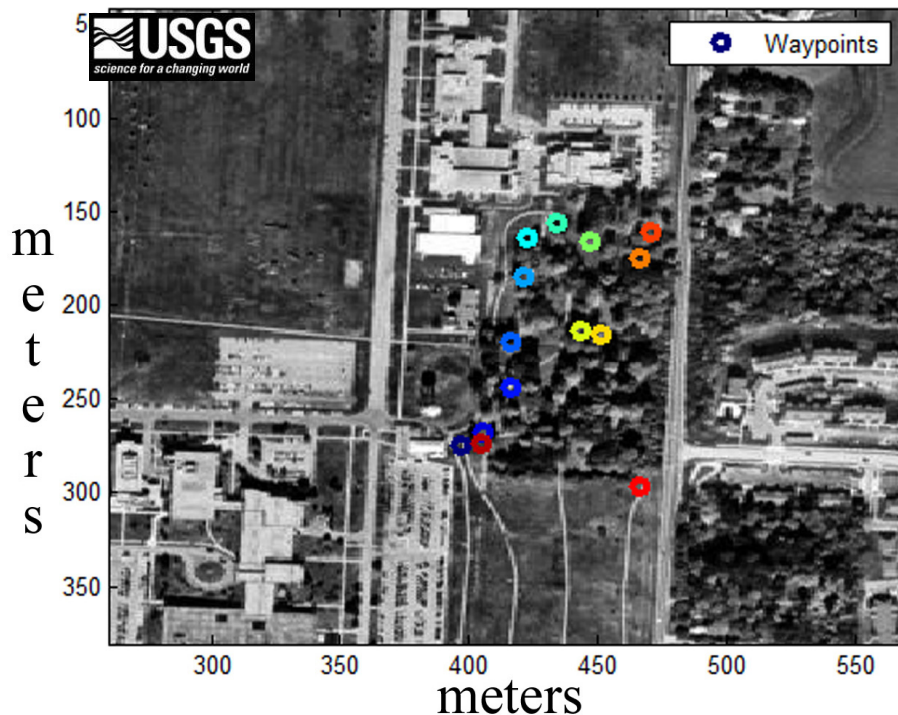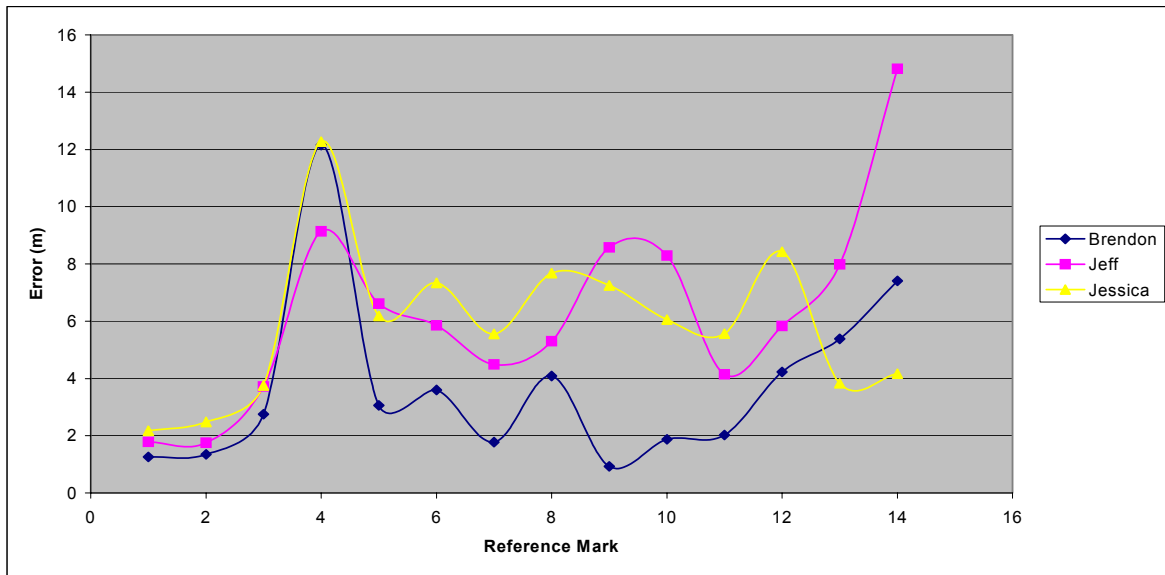

Figure 9. Surveyed reference points for forested scenario

Figure 10. Results for forest scenario

Table 2. Forest Final Error

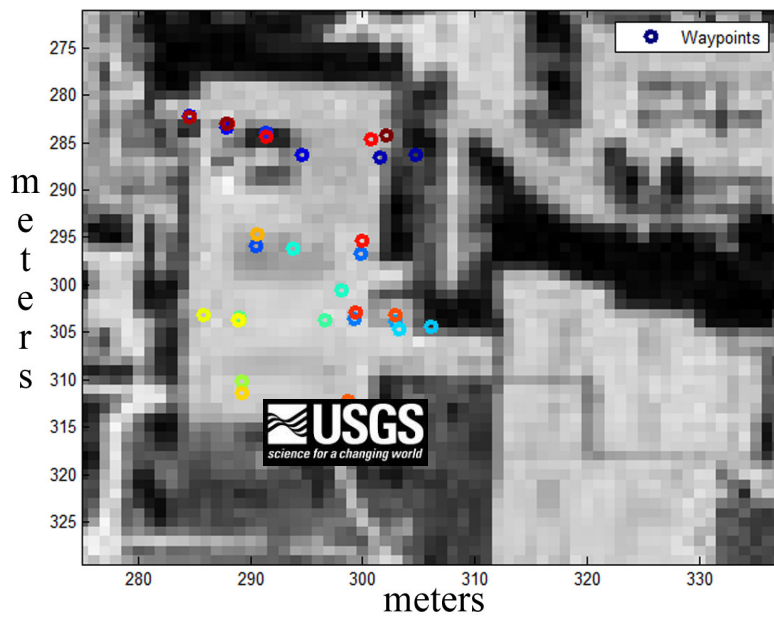| Test Subject	Final error	% Distance traveled (1100 meter)
Jeff	14.8 m	1.3 %
Jessica	4.2 m	0.38 %
Brendon	7.4 m	0.67 %

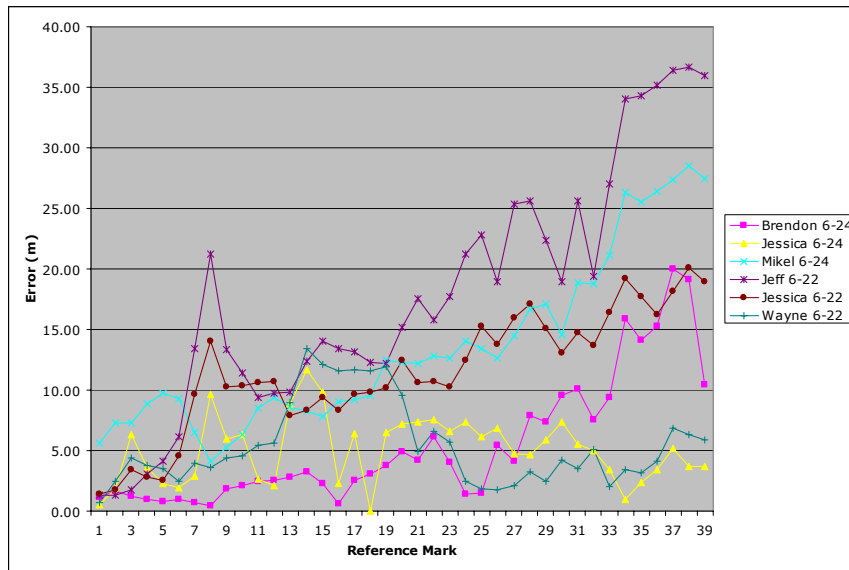**Figure 11. Surveyed reference points for indoor scenario**

Figure 12. Result summary for in-building scenario

Table 3. In-building Final Error

Test Subject	Final error (m)	% Distance traveled (1100 m)
Jeff 6-22	35.95	5.13 %
Jessica 6-22	18.92	2.7 %
Wayne 6-22	5.88	0.84 %
Brendon 6-24	10.45	1.49 %
Jessica 6-24	3.69	0.52 %
Mikel 6-24	27.47	3.92 %

4) Simulated terrain environment: Previous work in terrain correlation has shown a strong relationship of correlator accuracy with terrain slope variation. In this study, it was desirable to create terrain with controllable slope variation. Historically, statistically representative terrain has been created for simulation by using 1st or 2nd order Markov processes. However, the random nature of this process can create local terrain features that allow rapid correlator convergence, and can distort the relationship between correlator convergence and distance traveled. Since the primary interest of this study was in creating terrain with controlled slope variation, the approach taken was to generate terrain based on a simple analytical function, whose 1st and 2nd derivatives were easily computed. This led to a terrain generation function comprised of simple sine function, whose amplitude, cycle distance (frequency) and cycle offset (phase) were easily adjusted.

5) Barometric altitude sensor model: iPINS uses a barometric altitude sensor as the altitude measurement input to the terrain correlator. The iPINS barometric sensor was measured in actual use, and a model was chosen to represent the sensor's error characteristics. The model includes Gaussian random noise, 1st order Markov bias drift and 1st order Markov scale factor drift.

6) Simulated terrain map: Where the simulated trajectory is a continuous function, the associated terrain map is quantized to a fixed horizontal and vertical resolution. This horizontal quantization adds additional correlator noise, which is proportional to (terrain slope) x (horizontal resolution). The horizontal resolution of the simulated terrain map was selected to be 3 m., which corresponds to a DTED Level 4 resolution.

5.2   Position drift during correlation

The effect of position drift on the correlation surface is to introduce a moving "true" position relative to the map, which distorts the MAD surface minimum and adds ambiguity to the location of the minimum value location. This movement also tends to skew the MAD surface minimum toward terrain segments with the largest slope, potentially producing a bias. Since position drift error is independent of noise and slope change, and the non- linear nature of drift significantly complicates correlator performance analysis, position drift was not included as an error source in this study.

5.3   Correlator evaluation criteria

The MAD correlator produces a three-dimensional surface, as shown in Figure 13, whose magnitude is inversely proportional to the likelihood of the correct position. That is, the smallest MAD value of the surface is the most likely position of the navigator relative to the map. A measure of the ambiguity of the most likely position relative to the next most likely position is the numerical difference between the minimum value and the adjacent value.

Since, in the case of regular terrain, the correlation characteristic tends to be a symmetric cone, the average of the adjacent values is used in the difference calculation. To further simplify the problem and reduce the effect of correlated terrain in orthogonal directions, the correlation surface used was constrained to one dimension, along the direction of travel. Figure 14 depicts the correlation discriminator criteria.

5.4   Test Cases

This study investigated the suitability of terrain correlation as a positioning aid to the iPINS system. In general, terrain correlation accuracy is proportional to terrain slope change and correlation distance, and inversely proportional to altitude sensor noise. In aircraft applications, large amounts of terrain can be encountered in short periods of time, which reduces likelihood that unsuitable (flat) terrain is present for the duration of the correlation period, so performance is typically limited by map accuracy and sensor noise. For the iPINS case, the low speeds involved suggest that the accuracy limitation is more likely to be limited by terrain characteristics.
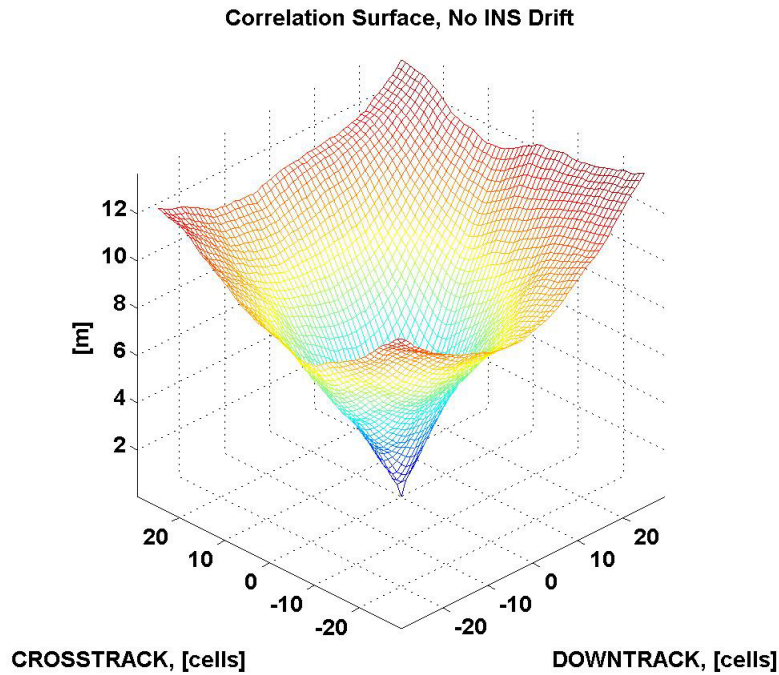
Correlation Surface, No INS Drift

Figure 13. Example correlation surface

For performance prediction, it was desirable to develop a relationship between sensor noise, terrain slope change and correlation length. A combination of the test conditions listed in Table 4 and Table 5 were in the simulation The duration of all simulation runs was 80 seconds, which corresponded to a linear distance of 100 meters.

Table 4. Slope Change Test Conditions

Slope Change (RMS)						
0.01	0.005	0.002	0.001	0.00005	0.0002	0.0001

Table 5. Altitude Sensor Noise Conditions

Altitude Sensor Noise (m)				
0.1	0.2	0.3	0.4	0.5

6.0   RESULTS

6.1   Relationship of correlator discriminator with correlation distance

The relationship of the correlator discriminator function to correlation distance was determined by periodically recording the correlation surface and computing and plotting the discriminator function. Figure 15 shows the correlation surface cross section in the direction of travel as a function of distance. The plot shows that the MAD minimum becomes more distinct relative to its neighboring points as the correlation distance increases; that is, the absolute value of the MAD function slope increases as the correlation distance increases.
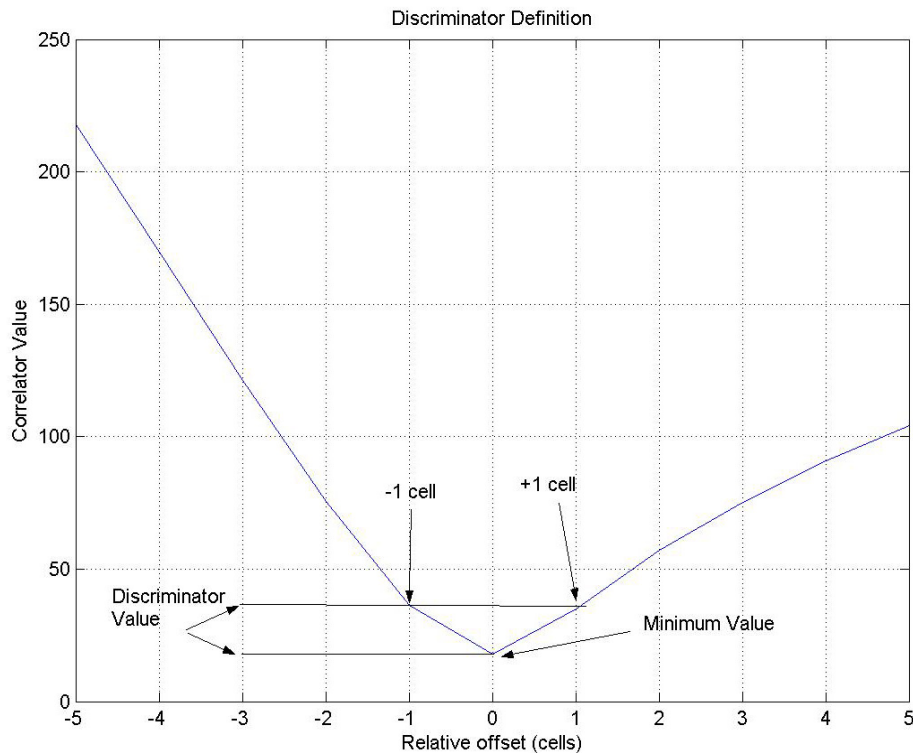
Figure 14. Correlation discriminator criteria

6.2   Relationship of correlator discriminator with sensor noise and slope variation

Figure 16 plots the discriminator function against time for several different altitude sensor noise values for a particular terrain slope profile. The plot shows that the discriminator function closely approximates a linear relationship with increasing distance, and that the slope of the plot varies with the applied noise level. Further analysis, using differing slopes and noise levels show an increased discriminator value with increasing slope, and suggest that a consistent relationship exists between the discriminator slope, terrain slope variation, sensor noise level and correlation distance.

6.3   Relationship of signal to noise ratio with correlation distance

An equivalent "signal to noise ratio" was sought to characterize the performance of the correlator under varying slope/noise conditions in terms of distance travelled. Since the discriminator function slope is positively correlated with increasing terrain slope change and negatively correlated with increasing sensor noise, a ratio composed of functions of slope variation/sensor noise was used in effort to find a relationship to discriminator slope. A relationship was found that predicts terrain correlation positioning performance in terms of terrain slope variation, correlation length and sensor noise. As an example of predicted performance, a typical scenario that includes a normal walking speed, a terrain slope variation of 0.005 and a correlation distance of <100 m yields a positioning accuracy of approximately 3m, when using a terrain map of 3m horizontal resolution.
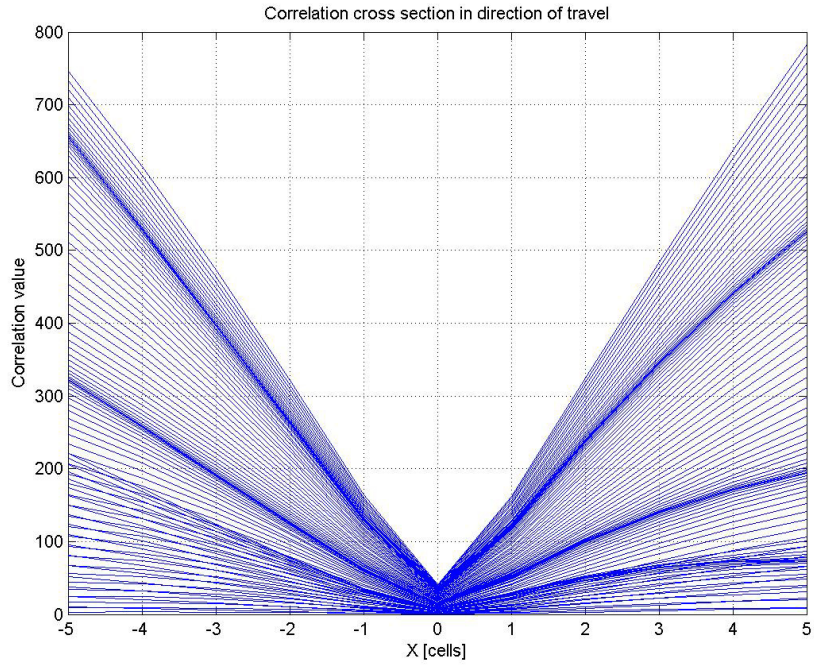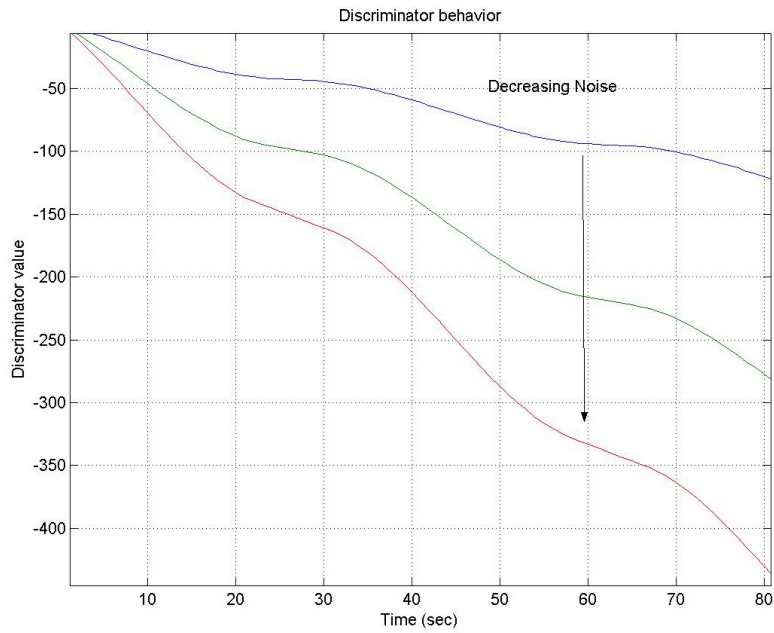
Figure 15. Correlator as a function of distance

Figure 16. Discriminator function behavior with distance and noise

7.0　CONCLUSIONS

The successful application of terrain navigation to personal navigation depends on the accuracy and frequency of terrain-based position updates. If the interval between position updates is too long or the accuracy not sufficient, position error may exceed acceptable limits. The accuracy of terrain correlation positioning primarily depends on 3 parameters: (1) Terrain slope change, (2) sensor noise, and (3) correlation distance. If the terrain is not suitable—that is the slope variation is too small compared with the altitude sensor noise —terrain correlation cannot be used successfully as a position aid. This study establishes a relationship for three parameters and can be used to predict when terrain correlation positioning can be successfully used. The example demonstrates that the barometric altitude sensor used in the iPINS system enables accurate correlation in a low slope variation scenario. This data indicates that terrain correlation positioning can be a useful method for bounding navigation error for a personal navigation application under a broad range of conditions.

8.0　ACKNOWLEDGMENTS

9.0　REFERENCES

[1]　Rodolfo Margaria. *Biomechanics and energetics of muscular exercise,* ch. 3, pp. 107-24. Oxford: Clarendon Press 1976.

[2]　US Patent 6,522,266 B1.　Navigation System, Method and software for Foot Travel. Issued Feb. 18, 2003.

[3]　US Patent Application 20050197769 Personal navigation using terrain-correlation and/or signal-of-opportunity information, filed 25/02/2005.